Design and Development of a Fluidic Barrier for Solar Cavity Receivers

Elham Alipour, Alfonso Chinnici, Zhao Tian , Gus Nathan, Bassam Dally

The Centre for Energy Technology
The University of Adelaide

Introduction

- Improvement of the competitiveness of Concentrated Solar Thermal (CST) technologies requires the innovations that advances the efficiency.
- The predominant CST technologies are parabolic troughs and solar towers.
- Convective heat losses contribute to about 60% of total losses from tower mounted cavity receivers.

➢ Parameters that affect the convective heat losses:
❖ Cavity geometry (aperture ratio, aspect ratio, shape, temperature);
❖ Cavity inclination and yaw angle;
❖ Wind seed.

➢ Methods to minimize the convective heat losses:
❖ Optimizing cavity design;
❖ Covering aperture with transparent material;
❖ Introducing aerodynamics barriers.

Methodology – Systematic Experimental Investigation

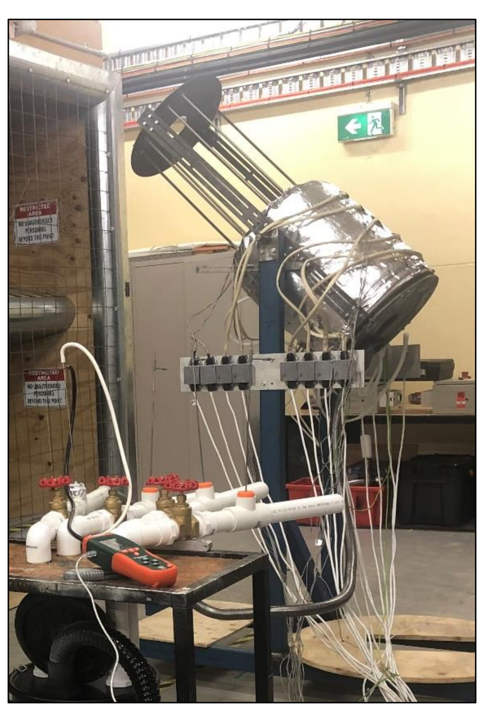

Electrically heated cavity

An electrically heated cylindrical cavity receiver placed in the open section of a large wind tunnel at various tilt angle and yaw angles.

Properties of the wind tunnel:
The cross-section of wind tunnel: 2.75 m × 2.19 m
The average air speeds of wind tunnel: u_w = 0, 3, 6 and 9 m/s

Definition of tilt angle θ and Yaw angle α

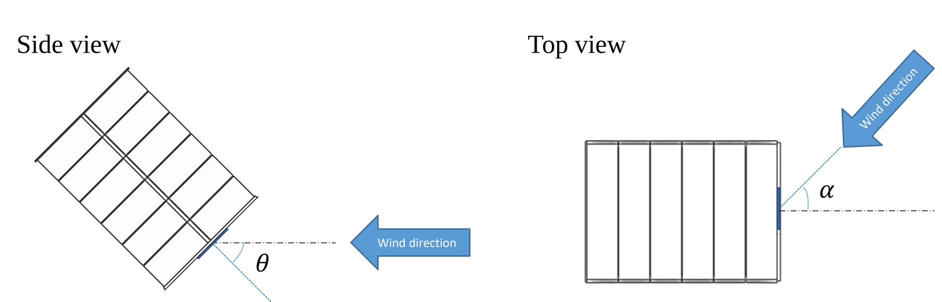

Configurations of blown air curtain

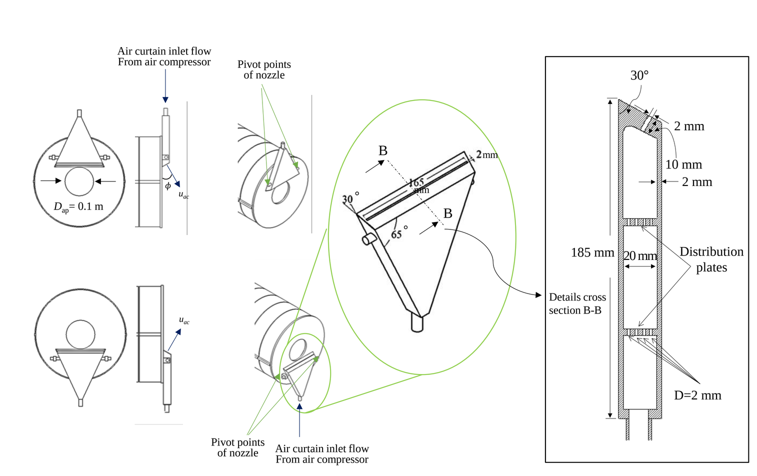

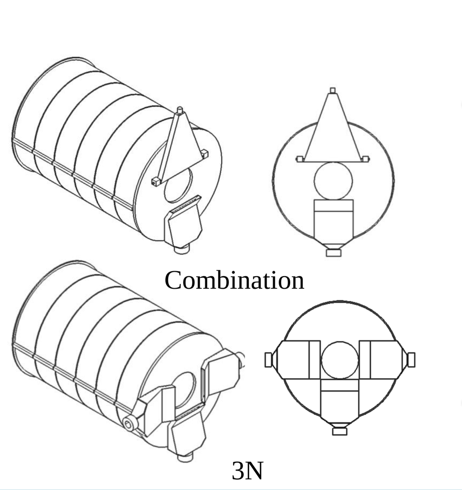

Configurations of Suction air curtain

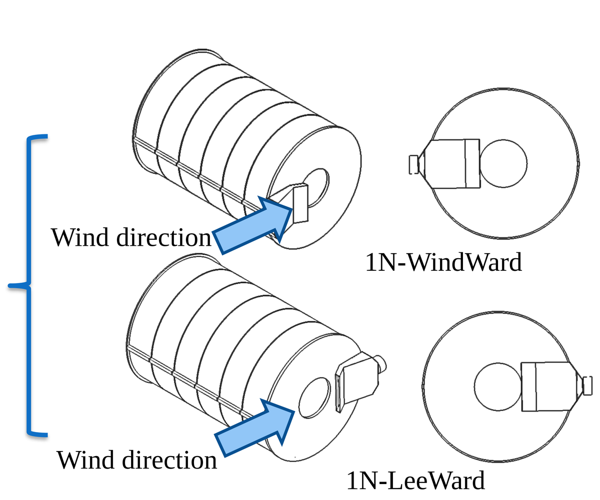

Methodology – Systematic Experimental Investigation

3-D computational fluid dynamics (CFD):
Software: ANSYS CFX 2020 R1
Method: the Reynolds-Averaged Navier-Stokes (RANS)
Meshing: non-uniform unstructured grid using ANSYS/Meshing 2020 R1
The working fluid: Air was (ideal gas, with the full "Buoyant" model)
The turbulence closure model: standard k-epsilon

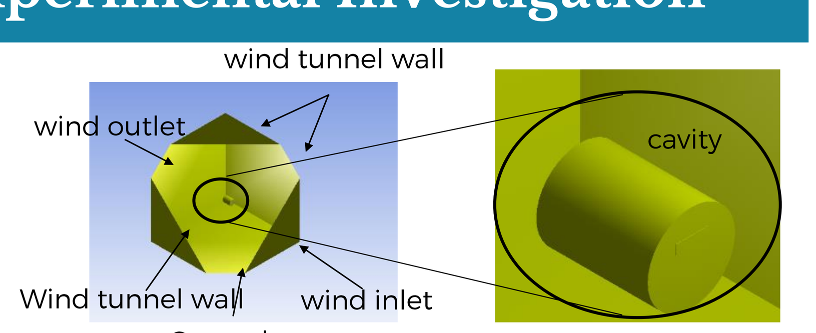

Geometry of the cavity and domain

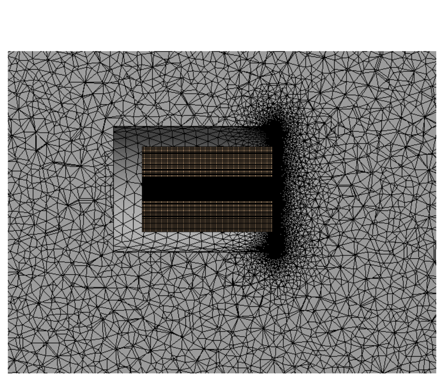

Mesh structure of the domain and internal volume of the cavity

Boundary	Condition
Cavity external walls	Adiabatic wall at 25℃
Domain walls	Wind inlet - Normal direction and uniform speed
	Wind outlet - Opening with relative pressure of 0 pa
	Ground - No-slip wall
	Sidewalls - Opening with relative pressure of 0 Pa
Cavity internal walls	No-slip wall - fixed temperature at 300 ℃
Air curtain- blowing	Inlet uniform velocity
Air suction	Outlet uniform velocity

Boundary conditions used for the numerical modelling

Results

Effect of curtain discharge angle, curtain velocity and wind speed

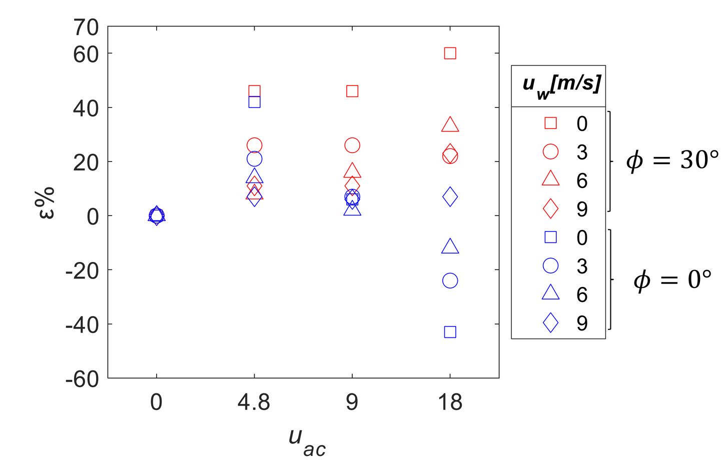

Comparison of the effectiveness of the air curtain for upward and downward orientation

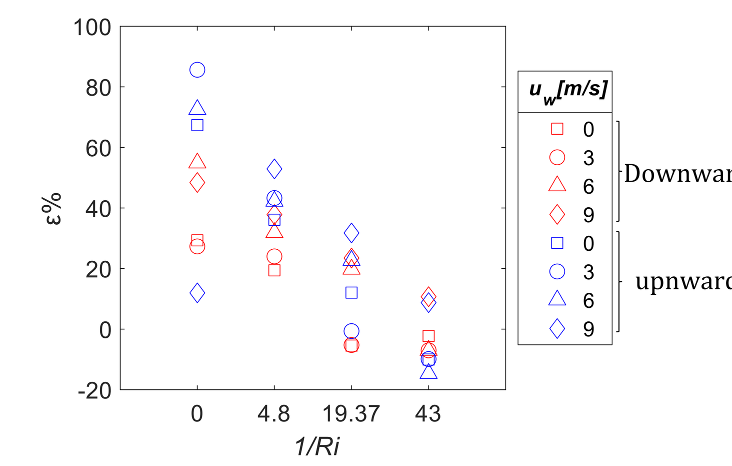

Modelled Temperature contours at the mid-plane of cavity for suction and blowing curtain at equal fan power – Buoyancy Dominated regime

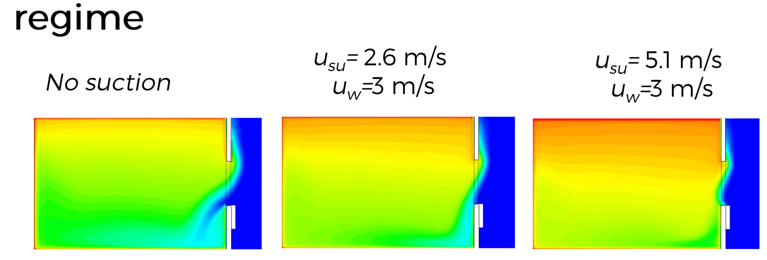

Modelled Temperature contours at the mid-plane of cavity at tilt angle of 0°.

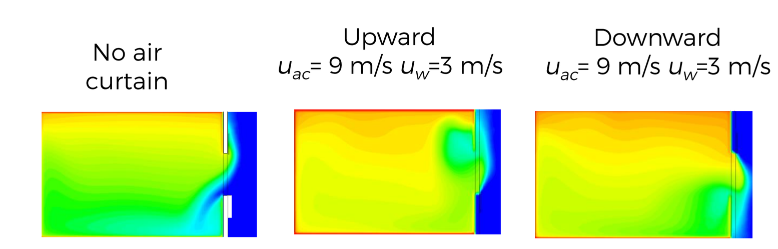

Effect of suction flowrate and inverse Richardson number for head-on wind

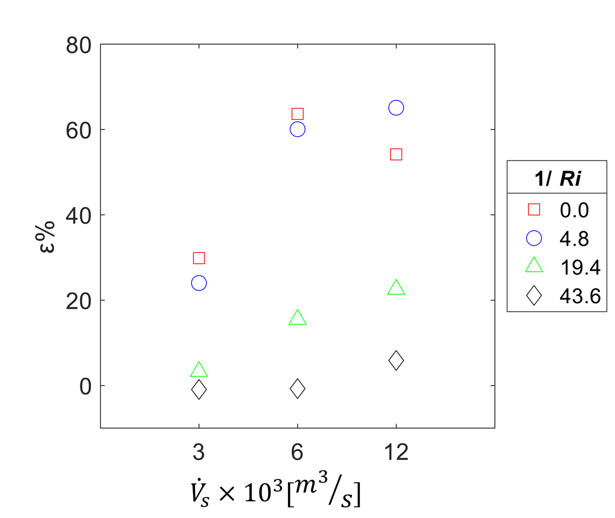

Effect of suction flowrate and inverse Richardson number for side on wind

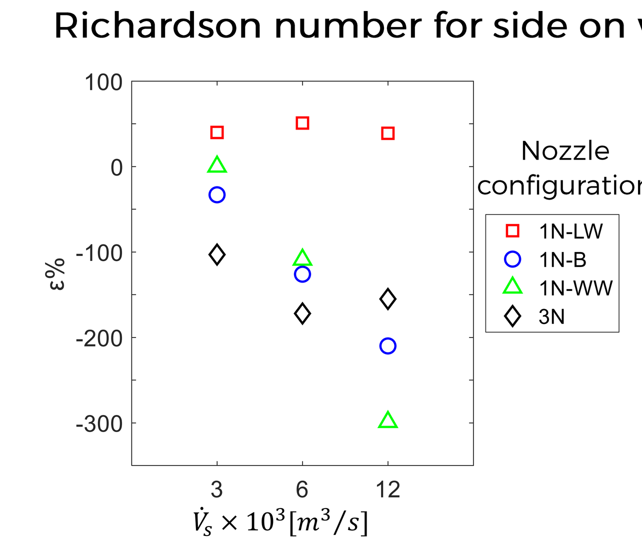

Effect of cavity tilt angle for suction

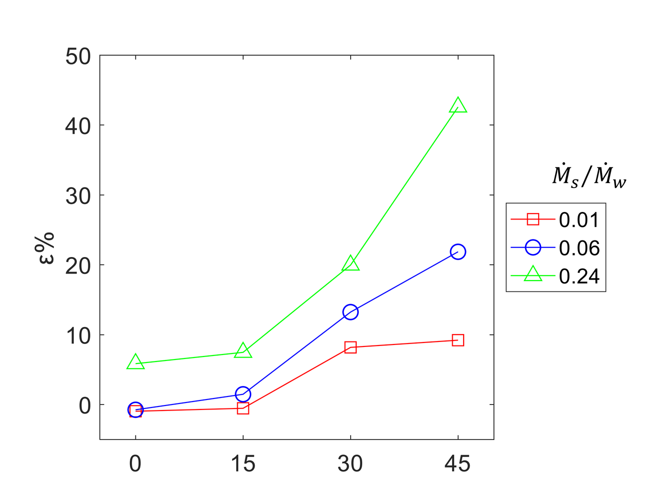

Effect of cavity tilt angle for blowing

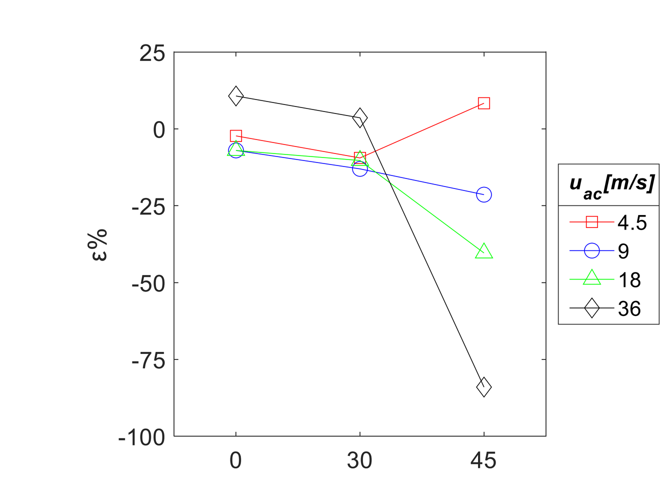

Combined curtain:

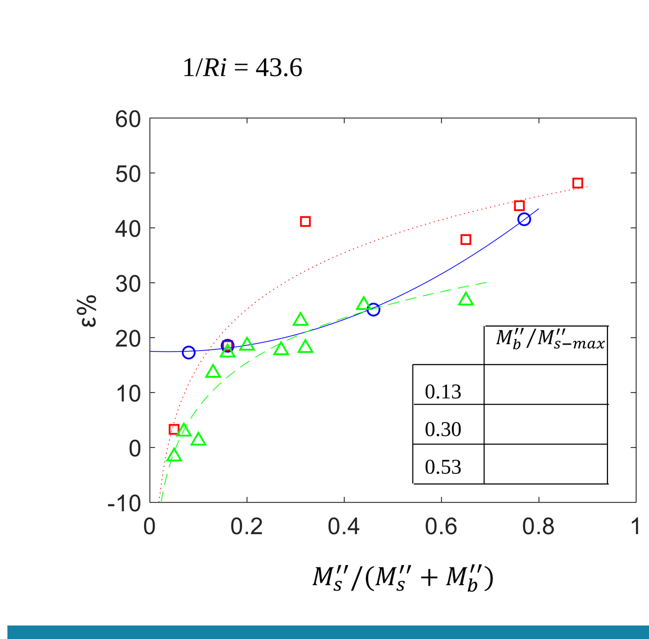

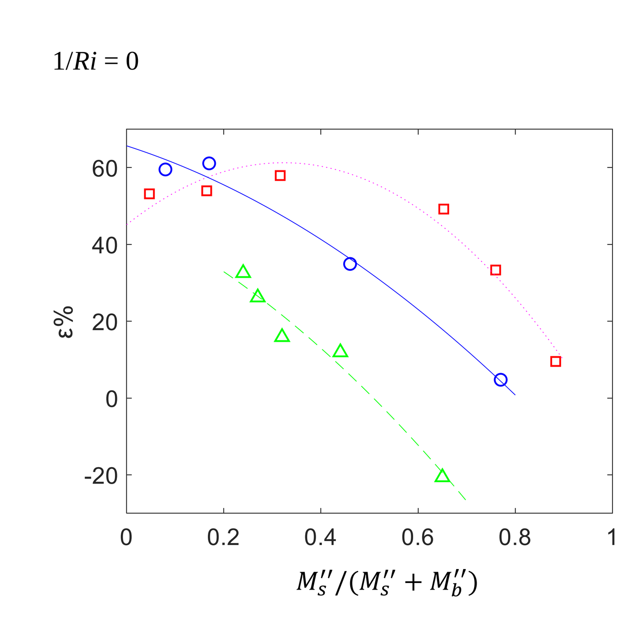

Conclusion

The results highlight the effect of velocity and discharge angle of the air curtain, tilt angle of the cavity, wind speed and wind direction on the effectiveness of the aerodynamic barrier. It is also found that the type and configurations of aerodynamic barrier has a major impact on the convective heat losses from solar cavity receivers.

It is concluded that an adaptive air curtain system should be devised so that it could sense the wind direction and wind speed and activate one or more of the curtain nozzles, induce suction or blowing, and regulate the air speed to achieve the best performance. This work provided the foundation for utilisation of a dynamic aerodynamic active flow for real world application of solar cavity receivers to improve the thermal efficiency of concentrating solar tower plants.

Acknowledgements

The authors would like to acknowledge the financial support of **ARENA** from grant 2015/RND054, from the **Australian Research Council** under grant LP110200060 and for the **Premier's Science and Research Fund** under grant 2007/1436.